Submitted to IEEE Guided Wave Letters

STUDY OF C_{max}/C_{min} RATIO ON THE PERFORMANCE OF BACK-TO-BACK BARRIER-N-N^+ (bbBNN) VARACTOR FREQUENCY MULTIPLIERS

DEBABANI CHOUDHURY, ANTTI V. RÄISÄNEN, R. PETER SMITH, MARGARET A. FRERKING

Center for Space Microelectronics Technology
Jet Propulsion Laboratory
California Institute of Technology
Pasadena, CA 91109

ABSTRACT

The effect of C_{max}/C_{min} ratio on the performance of planar back-to-back Barrier-N-N^+ (bbBNN) frequency multipliers is studied. A simplified physical model of the device is used to relate the electrical characteristics with the material and the structural parameters. Multiplication efficiency is evaluated using a large signal analysis approach. Results indicate that a high C_{max}/C_{min} ratio results in high efficiency.

I. INTRODUCTION

In order to improve the ruggedness of frequency multipliers for spaceborne local oscillator applications, planar varactor devices are being developed to replace whisker contacted devices. One candidate is the planar back-to-back Barrier-N-N^+ (bbBNN) varactor. It is a

modification of the Barrier-Intrinsic-N^+ (BIN) varactor [1], providing a lower series resistance. It exhibits a very sharp change in capacitance versus voltage characteristic, resulting in efficient harmonic generation at small input power levels. It has symmetric C-V and anti-symmetric I-V characteristics. Impedance nonlinearities symmetric to zero bias will generate only odd harmonics, thereby simplifying the mount design.

Previous studies on bbBNN and single barrier varactors [2,3,4] draw different conclusions on the impact of the C_{max}/C_{min} ratio on multiplier efficiency. In one case, the efficiency increased with C_{max}/C_{min} ratio [2], while in the other, it reached a maximum and then decreased [3,4]. In this paper, we study the effect of C_{max}/C_{min} ratio for two cases: (1) when C_{max} is held constant and (2) when C_{min} is held constant. In the first case, efficiency always increases with C_{max}/C_{min}. In the second case, the relationaship between C_{max}/C_{min} and efficiency is a function of input power level as well. Physically realizable device characteristics obtained from a simplified device model are used in a large signal analysis program to determine the RF performance.

II. DEVICE DESCRIPTION

A conceptual diagram of the bbBNN varactor is shown in Fig.1. The structure from the top surface down is; (i) Schottky contacts, separated by a gap, (ii) an AlGaAs layer that is sufficiently thick to preclude tunneling but sufficiently thin to allow large capacitance per unit area, (iii) a highly doped (delta doped) region which introduces a built-in potential to ensure that the high capacitance mentioned above is achieved at zero voltage, (iv) a moderately doped GaAs depletion region, and (v) a highly doped region that provides a low resistance path between the two metal contact pads. The layer thicknesses, doping densities and compositions can be adjusted

for optimum performance. The operation of the device as a varactor is described in references [2,5].

III. PHYSICAL DEVICE MODELING

We have theoretically designed several physically realizable devices having different C_{max}/C_{min} ratios. These devices are summarized in Table-I, which includes device dimension (illustrated in Fig.1) and doping parameters as well as the series resistance, the breakdown voltage and cut-off frequencies. To calculate device parameters, the depletion approximation was used. In addition, the three-dimensionality inherent to the back-to-back varactor was ignored. This assumption, neglecting fringing and parasitic capacitances, results in a lower minimum capacitance than is observed in real varactors.

Tables-I(a,b) show characteristics for $8\mu m^2$ area devices with $2\mu m$ wide Schottky contacts across $4\mu m$ wide mesas and $2\mu m$ separation between contacts. These dimensions are typical for those used in a 67 to 200 GHz tripler [6]. Tables-I(c,d) show characteristics for $4\mu m^2$ area devices with $1\mu m$ wide Schottky contacts. To assess the impact of the capacitance ratio C_{max}/C_{min} on efficiency, several devices for each area are considered. In Table-I(a), C_{max} is constant at 30 fF, while the ratio C_{max}/C_{min} is varied between 5 and 2. In Table-I(b), C_{min} is constant at 7.5 fF, while C_{max} is adjusted to vary the ratio of C_{max}/C_{min}. In Table-I(c), C_{max} is constant at 15 fF, since the area is a factor of 2 smaller than the device in Table-I(a). Similarly, in Table-I(d), C_{min} is constant at 3.75 fF.

C_{max} is determined by the barrier thickness, x_b and the device area. The ratio of C_{max}/C_{min} sets the depletion region thickness x_d. The δ-doping, n_s and depletion region doping N_d were adjusted so that, the voltage necessary to completely deplete the depletion region is held constant

at 2.32V.

The total series resistance R_s is given by,

$$R_s = R_d + R_n + R_p, \quad (1)$$

where R_d is the resistance of the depletion region, R_n is the resistance of the n^+ region and R_p is the parasitic metal resistance. The depletion region resistance R_d and the resistance due to the n^+ region, R_n are given by,

$$R_d = (1.5 \cdot x_d)/(L \cdot W \cdot q \cdot \mu_d \cdot N_d), \quad (2)$$

and

$$R_n = (L+x_g)/(W \cdot x_n \cdot q \cdot \mu_n \cdot N_n), \quad (3)$$

where x_d and x_n are the thicknesses, N_d and N_n are the doping densities and μ_d and μ_n are the mobilities of the depletion region and the n^+ region respectively. L is the length of the metal pad, W is the width of the metal pad and x_g is the gap between the metal pads (Fig.1). The factor 1.5 in R_d is used to approximate an average resistance over one cycle since depletion region width is a function of applied voltage and varies throughout the pump cycle. The mobilities of the depletion and n^+ regions are assumed to be 0.4 and 0.2 m^2/V-s, respectively. The parasitic metal resistance R_p due to the Ti/Pt/Au fingers was calculated to be 0.67 Ω and 1.3 Ω, for 8μm^2 and 4μm^2 device areas, repectively. The series resistance values of 7-12 Ω are in reasonable agreement with measurements [6]. The resistance of the n^+ region is the dominating part in the series resistance values.

The breakdown voltage V_{bd}, modeled here, is due to Fowler-Nordheim tunneling [5]. Devices made in the laboratory have always shown lower breakdown voltages than the modeling indicates. This may be due to an avalanche mechanism.

The cut-off frequency associated with the RC time constant of the device was determined

by the formula

$$f_{c\text{-}RC} = \frac{1}{2\pi R_s}\left(\frac{1}{C_{min}} - \frac{1}{C_{max}}\right), \qquad (4)$$

where R_s is the resistance modeled at zero bias.

IV. LARGE SIGNAL ANALYSIS

The effect of C_{max}/C_{min} on bbBNN varactor tripler efficiency from 67 GHz to 200 GHz was evaluated for the devices in Table-I, using a modified version of the nonlinear program by Siegel et al. [7]. The importance of low series resistance has been described earlier [6]. Embedding network impedances at the input and output frequencies were optimized. Other harmonic embedding impedances were assumed to be open circuited. The effect of electron velocity saturation [8] have not been included and will reduce the performance for high pump powers and high frequencies.

The results are shown in Fig.2, where the tripling efficiency is plotted as a function of input power parameterized by the C_{max}/C_{min} ratio. Figs.2(a) and (b) are the results for bbBNN with areas of 8 μm^2; Figs.2(c) and (d) are for 4 μm^2 device area. In Figs.2(a) and (c), the maximum capacitance has been held constant, while in Figs.2(c) and (d) the minimum capacitance is constant.

As can be seen in Fig.2, the peak efficiency is highest for the device with highest $f_{c\text{-}RC}$. The pump power at which the peak efficiency is obtained depends primarily on C_{max} since the voltage to completely deplete the depletion region is fixed for all cases presented here. Hence, the 8 μm^2 device [Figs.2(a) and (b)] requires more pump power for peak efficiency than the 4

μm^2 device [Figs.2(c) and (d)]. In the case, where C_{max} is fixed [Figs.2(a) and (c)], the pump power for peak efficiency is roughly constant. However, in the case when C_{min} is fixed [Figs.2(b) and (d)] and C_{max} varies, the pump power for peak efficiency increases with C_{max} and hence with the C_{max}/C_{min} ratio.

V. CONCLUSION

From the above simulations, the previous discrepancy on the impact of C_{max}/C_{min} ratio can be understood. In one case [2], the C_{max} was fixed, whereas in the other case [3], C_{min} was fixed. When C_{max} is fixed, the efficiency is always improved with high C_{max}/C_{min}. For the fixed C_{min} case, if a low input power (for the cases studied here below about 5 mW) was also assumed, the efficiency would appear to peak for an intermediate C_{max}/C_{min} ratio. This is especially true if the diode area is large. But if a higher input power (10 mW or more) is used with the optimum device size for the given frequency, the highest possible C_{max}/C_{min} ratio results in maximum efficiency. Thus a "rule of thumb" is that the highest cut-off frequency, $f_{c\text{-}RC}$ and the highest C_{max}/C_{min} gives the best multiplication efficiency.

ACKNOWLEDGEMENTS

The research described in this paper was carried out at the Center for Space Microelectronics Technology, Jet Propulsion Laboratory, California Institute of Technology, under contract with the National Aeronautics and Space Administration, Office of Aeronautics, Space

and Technology.

REFERENCES

1] U.Lieneweg, B.R.Hancock and J.Maserjian, 'Barrier-Intrinsic-n^+ (BIN) diodes for near-millimeter wave generation,', Proceedings of 12th International Conference of Infrared and Millimeter Waves, pp.6-7, 1987.

2] M.A.Frerking and J.R.East, 'Novel heterojunction varactors', Proceedings of IEEE, vol.80, no.11, pp.1853-1860, Nov.1992.

3] H.Grönqvist, S.M.Nilsen, A.Rydberg and E.Kollberg, 'Characterizing highly efficient millimeter wave single barrier varactor multiplier diodes', Proceedings of the 22nd European Microwave Conference (Espoo, Finland), pp.479-484, August 1992.

4] S.M.Nilsen, H.Grönqvist, H.Hjelmgren, A.Rydberg and E.Kollberg, 'Single barrier varactors for submillimeter wave power generation', IEEE Trans. on Microwave Theory and Techniques, vol.41,no.4,pp.572-580, May 1992.

5] U.Lieneweg, T.J.Tolmunen, M.Frerking and J.Maserjian, 'Design of planar varactor frequency multiplier devices with blocking barriers', IEEE Trans. on Microwave Theory and Techniques, vol.40,no.5,pp.839-845, May 1992.

6] D.Choudhury, A.V.Räisänen, R.P.Smith, M.A.Frerking, S.C.Martin and J.K.Liu, 'Experimental performance of a back-to-back barrier-N-N^+ (bbBNN) varactor tripler at 200 GHz', accepted for publication in IEEE Trans. Microwave Theory and Techniques, April 1994.

7] P.H.Siegel, A.R.Kerr and W.Hwang, 'Topics in the optimization of millimeter wave mixers', NASA Tech. paper 2287, 1984.

8] E.L.Kollberg, T.J.Tolmunen, M.A.Frerking and J.R.East, 'Current saturation in submillimeter-wave varactors', IEEE Trans. on Microwave Theory and Technique, vol.40, no.5, pp831-838, 1992.

FIGURE CAPTIONS

1. Schematic diagram of a back-to-back BNN varactor.

2. Tripling efficiency versus input power plot for 67 to 200 GHz tripler parameterized by C_{max}/C_{min} and cut-off frequency associated with the RC-time constant of the device

   (a) C_{max}=30 fF, variation of C_{min} (device area = 8 μm^2),

   (b) C_{min}=7.5 fF, variation of C_{max} (device area = 8 μm^2),

   (c) C_{max}=15 fF, variation of C_{min} (device area = 4 μm^2),

   (c) C_{max}=3.75 fF, variation of C_{max} (device area = 4 μm^2).

LIST OF TABLES

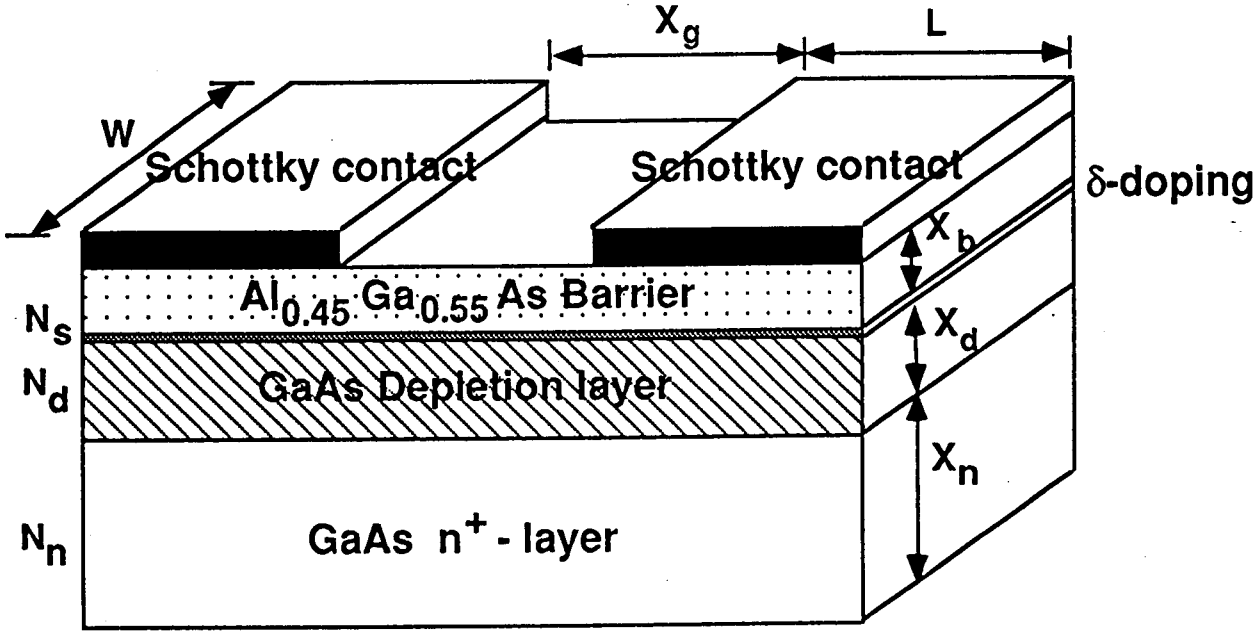
X_g
L
W
Schottky contact
Schottky contact
δ-doping
X_b
$Al_{0.45}Ga_{0.55}As$ Barrier
N_s
X_d
N_d
GaAs Depletion layer
X_n
N_n
GaAs n^+ - layer

Fig. 1

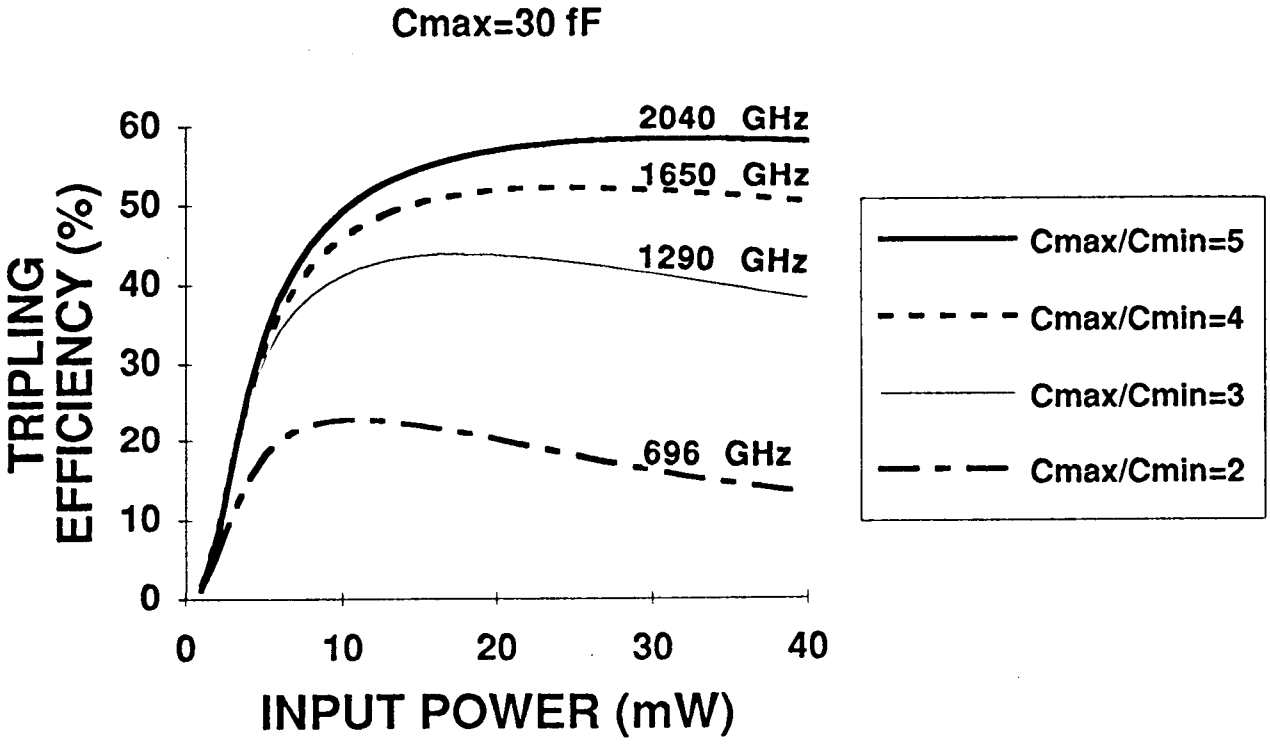
Cmax=30 fF
TRIPLING EFFICIENCY (%)
60
50
40
30
20
10
0
0
10
20
30
40
INPUT POWER (mW)
2040 GHz
1650 GHz
1290 GHz
696 GHz
Cmax/Cmin=5
Cmax/Cmin=4
Cmax/Cmin=3
Cmax/Cmin=2

Fig. 2a

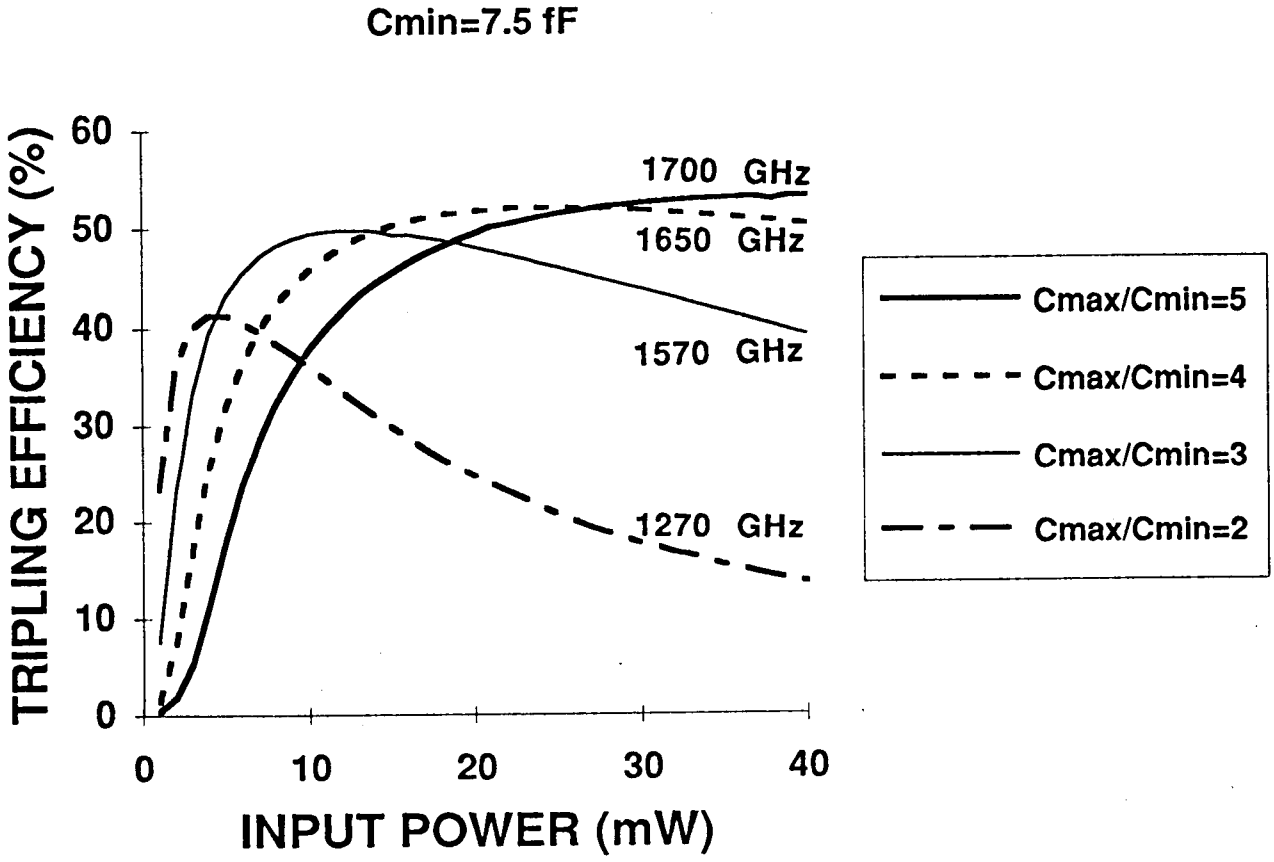
Cmin=7.5 fF
TRIPLING EFFICIENCY (%)
60
50
40
30
20
10
0
0
10
20
30
40
INPUT POWER (mW)
1700 GHz
1650 GHz
1570 GHz
1270 GHz
Cmax/Cmin=5
Cmax/Cmin=4
Cmax/Cmin=3
Cmax/Cmin=2

Fig 2b

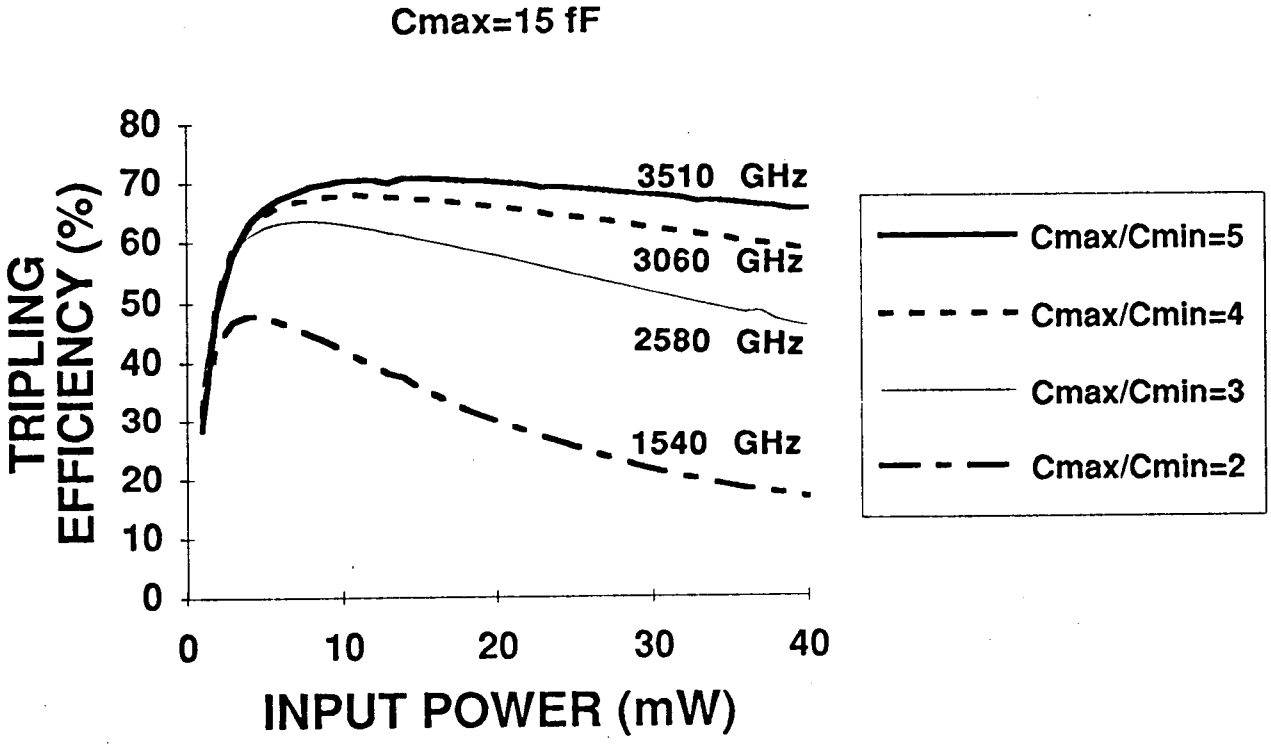
Cmax=15 fF
TRIPLING EFFICIENCY (%)
80
70
60
50
40
30
20
10
0
0
10
20
30
40
INPUT POWER (mW)
3510 GHz
3060 GHz
2580 GHz
1540 GHz
Cmax/Cmin=5
Cmax/Cmin=4
Cmax/Cmin=3
Cmax/Cmin=2

fig. 2c

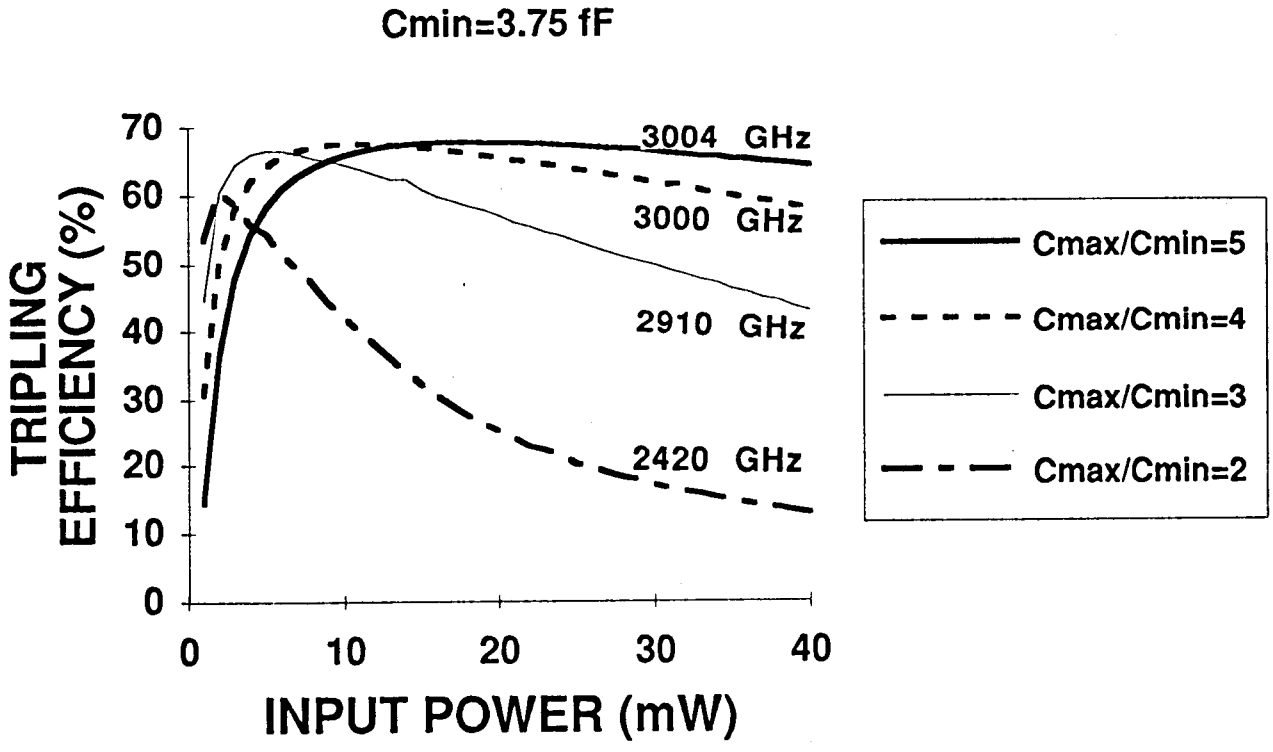
Cmin=3.75 fF
TRIPLING EFFICIENCY (%)
70
60
50
40
30
20
10
0
0
10
20
30
40
INPUT POWER (mW)
3004 GHz
3000 GHz
2910 GHz
2420 GHz
Cmax/Cmin=5
Cmax/Cmin=4
Cmax/Cmin=3
Cmax/Cmin=2

Fig. 2d.

Table I

(a) C_{max} = 30 fF, device area = 8 μm^2							
$\frac{C_{max}}{C_{min}}$	x_b (nm)	x_d (nm)	n_s (cm^{-2})	N_d (cm^{-3})	R_s (Ω)	V_{bd} (volts)	f_{cRC} (GHz)
5	15.3	122.5	2.95×10^{12}	1.30×10^{17}	10.4	23.5	2040
4	15.3	92.0	6.00×10^{12}	1.33×10^{17}	9.6	14.5	1650
3	15.3	61.0	5.00×10^{12}	3.24×10^{17}	8.2	11.5	1290
2	15.3	31.0	5.00×10^{12}	9.46×10^{17}	7.7	7.4	696
(b) C_{min} = 7.5 fF, device area = 8 μm^2							
$\frac{C_{max}}{C_{min}}$	x_b (nm)	x_d (nm)	n_s (cm^{-2})	N_d (cm^{-3})	R_s (Ω)	V_{bd} (volts)	f_{cRC} (GHz)
5	12.3	98.1	7.70×10^{12}	1.20×10^{17}	10.0	12.3	1700
4	15.3	90.0	6.00×10^{12}	1.33×10^{17}	9.6	14.5	1650
3	20.4	81.9	4.00×10^{12}	1.70×10^{17}	9.0	16.6	1570
2	30.6	61.5	2.53×10^{12}	2.37×10^{17}	8.4	16.9	1270
(c) C_{max} = 15 fF, device area = 4 μm^2							
$\frac{C_{max}}{C_{min}}$	x_b (nm)	x_d (nm)	n_s (cm^{-2})	N_d (cm^{-3})	R_s (Ω)	V_{bd} (volts)	f_{cRC} (GHz)
5	15.3	122.5	2.95×10^{12}	1.30×10^{17}	12.0	23.5	3510
4	15.3	92.0	5.75×10^{12}	1.40×10^{17}	10.4	14.8	3060
3	15.3	61.5	7.00×10^{12}	2.10×10^{17}	8.3	9.9	2580
2	15.3	30.7	7.85×10^{12}	5.00×10^{17}	6.9	6.2	1540
(d) C_{min} = 3.75 fF, device area = 4 μm^2							
$\frac{C_{max}}{C_{min}}$	x_b (nm)	x_d (nm)	n_s (cm^{-2})	N_d (cm^{-3})	R_s (Ω)	V_{bd} (volts)	f_{cRC} (GHz)
5	12.3	98.1	7.70×10^{12}	1.20×10^{17}	11.3	12.3	3004
4	15.3	92.0	6.00×10^{12}	1.33×10^{17}	10.6	15.0	3000
3	20.4	81.9	4.50×10^{12}	1.50×10^{17}	9.7	16.0	2910
2	30.7	61.5	3.48×10^{12}	1.60×10^{17}	8.8	16.0	2420